

ELECTRORHEOLOGICAL FLUID POWER REQUIREMENTS FOR AN ADAPTIVE TUNABLE VIBRATION ABSORBER

Nicklas Norrick*¹

¹Institute of Structural Dynamics, Technische Universität Darmstadt
Petersenstr. 30, 64287 Darmstadt, Germany
norrick@sdy.tu-darmstadt.de

Keywords: Electrorheological Fluid, ERF, Tuned Vibration Absorber, Semi-Active

Abstract. *Electrorheological fluid (ERF) is an adaptive material which changes its physical characteristics quickly and reversibly in response to an electric field, first shown by Winslow in 1947. This change in behavior makes it possible to influence the natural frequencies and damping of a multibody tuned vibration absorber (TVA) filled with ERF. In this paper, an adaptive multibody absorber prototype is investigated. Its performance is evaluated numerically and experimentally with special focus on power requirements and efficiency of the semi-active tuning mechanism. The multibody TVA prototype consists of a closed casing, in which two rigid bodies are suspended via helical springs. Two independent high-voltage channels allow the application of high voltages of up to 6000 V to influence the ER material in the narrow gaps between the absorber bodies. Experiments show that it is possible to continuously change the apparent natural frequencies and damping of the absorber. A nonlinear mathematical model of the prototype which has been validated using the experimental results is presented. An extended BINGHAM model is used to describe the behavior of the ERF under influence of an electric field. Using the validated numerical model, the power dissipation in the absorber can be calculated and compared to the measured power requirements of the ERF as well as the power consumption of the high voltage amplifiers. The efficiency of the ER material as a semi-active tuning mechanism is shown to be very high in contrast to active solutions for vibration absorbers. This information can help foster further developments of adaptive TVAs utilizing ERF as an adjustment mechanism.*

1 INTRODUCTION

Electrorheological fluid (ERF) is an adaptive material which can be used to influence dynamic systems such as tuned vibration absorbers (TVAs). It is well-known that the classical TVA is only capable of quenching vibrations at its tuning frequency [1]. Using ERF, the natural frequency and damping characteristics of a multibody tuned vibration absorber can be changed to achieve vibration attenuation over a broad frequency band. This can be of special interest when the excitation frequencies of a system vary during operation.

The adaptive TVA is a semi-active device according to Preumont's definition [2], which has certain advantages over active systems. First, semi-active devices require very little energy in comparison with an active system. Second, since semi-active devices cannot input energy directly into the system they are used in, the robustness of the device in the case of a failure in the control system is comparable to passive solutions. A comparison of passive, semi-active and active TVA performance can be found in [3].

Since the discovery of the electrorheological effect by Winslow almost seventy years ago [4, 5], much research has been done using ERF as a smart material in dynamic systems. For example Bullough and Foxon [6] use adaptive dampers for the control of unwanted vibrations. Magnetorheological fluids (MRF) utilize the magnetorheological effect for very similar changes in material behavior and have been studied extensively as well for the use in adjustable dampers. Recent work by Sims et al. [7] is one example.

For tunable vibration absorbers, some experimental and theoretical work has been done using same change in material behavior, either with ERF or MRF. Janocha and Jendritza [8] presented a prototype absorber with adjustable damping characteristics utilizing electrorheological fluid. Sloshing-type vibration absorbers have been studied by both Truong and Semercigil [9] and Sakamoto et al. [10]. In both cases, experimental results were obtained using ERF as a sloshing liquid in a tank. Truong and Semercigil noted a change in the damping of the TVA while Sakamoto et al. proved that it is possible to change the effective mass of the absorber and thereby influence the tuning frequency. Koo [11] used MRF dampers to design a semi-active TVA and presented theoretical and experimental results showing the semi-active system's significant advantages over classical TVAs. Magnetorheological elastomers (MRE) were implemented by Holdhusen [12] to create a semi-active TVA with adaptive stiffness, which also showed good performance compared with passive systems. Also, several research groups have discussed the possibility of changing a sandwich beam's stiffness with ERF or MRF and done extensive theoretical and experimental work. Only recently has this stiffness-changing effect been used to change TVA properties on-line by Hirunyapruk [13].

An existing adaptive multibody TVA prototype is the subject of this paper. In previous work, it has been proven that the natural frequencies and damping of this prototype can be adapted semi-actively by applying high voltages of up to 6000 V [14, 15] in gaps of ~ 1 mm, resulting in electrical field strengths of up to 6 kV/mm. The prototype has also been applied to an automobile substructure and measurements have been made to validate its performance. To quantify the advantage of a semi-active TVA compared to fully active solutions, this paper concentrates on the power consumption and efficiency (defined as the ratio of power dissipation of the "smart" material to its power consumption) of the mentioned prototype.

2 MULTIBODY TVA PROTOTYPE

The prototype TVA investigated in this study consists of a closed casing, in which two bodies are suspended via helical springs. The coupling body (mass m_1), has only 10% of the mass of

the main body (mass m_2). In the narrow gaps between the coupling body and the casing a high voltage U_1 can be applied, while in the narrow gaps between the coupling body and the main body a different high voltage U_2 can be applied. Both voltages are supplied by independently controlled high voltage amplifiers, each up to 6000 V. The casing of the absorber is filled with ERF under a slight overpressure to prevent the formation of air bubbles, which have a negative effect on the dielectric strength of the material. The size of the prototype enables the fitting of the absorber into the steering wheel of a luxury automobile. Figure 1 shows a photograph of this prototype.

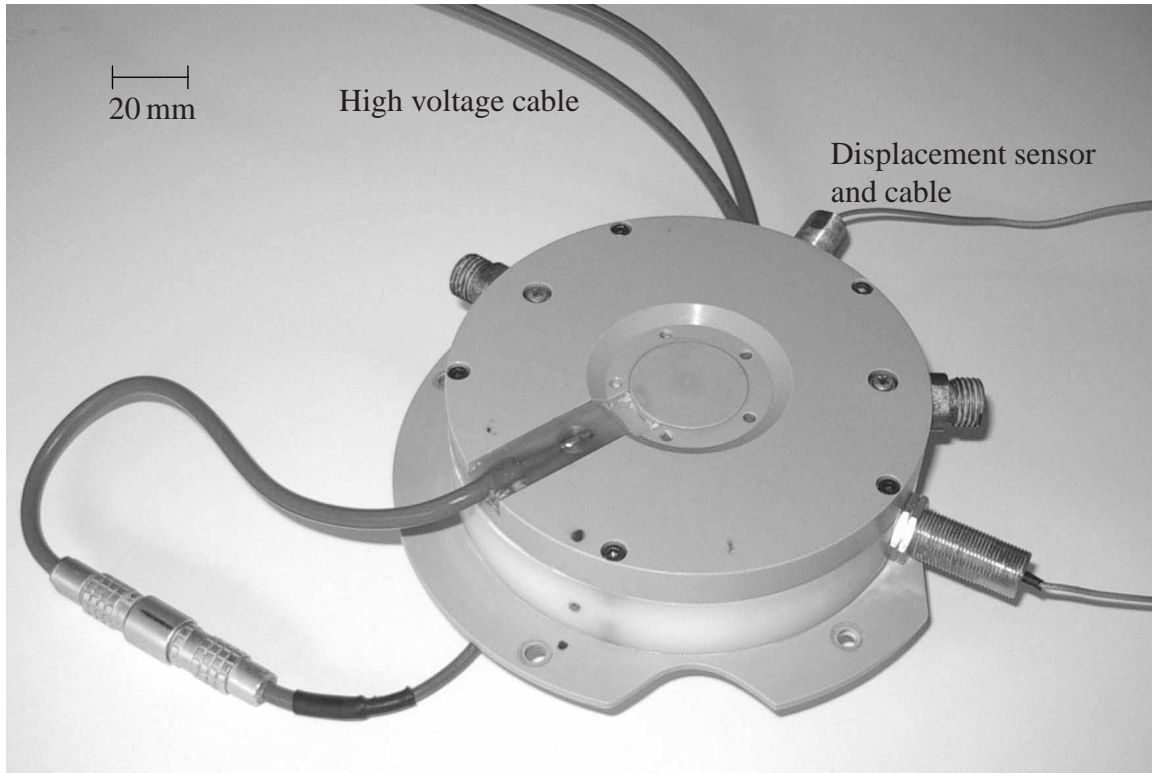


Figure 1: Photograph of the multibody tunable vibration absorber prototype

3 MATHEMATICAL MODEL

An idealized mechanical model of the absorber is shown in Figure 2. The application of the high voltage U_1 or U_2 influences the ERF and can achieve a blockage of the spring-damper set 1 or 2, respectively, thereby influencing system damping and natural frequencies.

To model the influence of the ERF, a nonlinear extended BINGHAM-type model based on viscometer measurements is used. The model parameters are the electric field strength E_{el} and the shear rate $\dot{\gamma}$. The shear stress τ_{ERF} is the sum of the field-dependent yield stress τ_y and a viscous part,

$$\tau_{ERF}(E_{el}, \dot{\gamma}) = \tau_y(E_{el}) + \mu(E_{el}) \dot{\gamma} \quad (1)$$

The yield stress τ_y must be exceeded for motion to occur. The values of $\tau_y(E_{el})$ and $\mu(E_{el})$ are determined by fitting the model to the aforementioned viscometer measurements (crosses in Figure 3a) using the least-square method for electrical field values from 0 to 6 kV/mm.

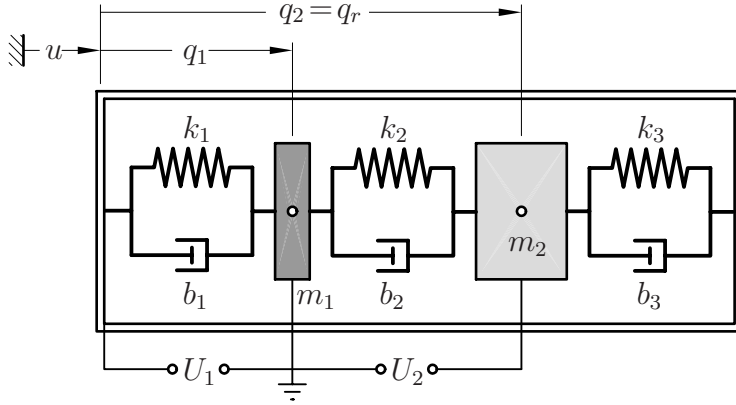


Figure 2: Sketch of the multibody tunable vibration absorber model

The shear rate is assumed to be directly proportional to the shear stress, consistent with the assumption of a NEWTONIAN Fluid. Because the energy density in an electrical field

$$e_{el} = \frac{1}{2} \varepsilon \varepsilon_0 E_{el}^2, \quad (2)$$

is proportional to the square of the electrical field strength a quadratic ansatz for the influence of the electrical field strength on the shear stress is plausible [16]. The equations

$$\tau_y(E_{el}) = a_\tau E_{el}^2 \quad \text{and} \quad \mu(E_{el}) = \mu_0 + a_\mu E_{el}^2 \quad (3)$$

are used. The result of the fitting of the model to the viscometer measurements is shown in Figure 3 on the left.

Extensive measurements at the Institute of Structural Dynamics at the Technische Universität Darmstadt [17] have shown that there is no hard transition to the flowing of the ERF, as the basic BINGHAM-model suggests. To account for this, the arctan-function is used to smooth the jump in the shear stress at the shear rate $\dot{\gamma} = 0$. This form function has the additional advantage that numerical simulations do not have to cope with the discontinuity presented by the BINGHAM-model. In Figure 3 on the right is a zoom of the area where the influence of the arctan-function is clearly visible. The shear stress is now given by

$$\tau_{ERF}(E_{el}, \dot{\gamma}) = [\tau_y(E_{el}) + \mu(E_{el}) \dot{\gamma}] \frac{2}{\pi} \arctan\left(c \frac{\dot{\gamma}}{\dot{\gamma}_{max}}\right), \quad (4)$$

so that the electrode area A can then be used to calculate a resulting ERF force. In our case, the effective electrode area $A = 8657 \text{ mm}^2$. The enclosed area in a force-displacement diagram is the damping work done by one vibration cycle. Multiplication of the damping work with the frequency (in Hz) yields the damping power (in W).

The shown model for the semi-active tuned vibration absorber and the electrorheological material has been parameterized and validated by vibration response measurements with different types of excitation [18]. The model reproduces the measured dynamic behavior of the absorber under influence of applied high voltage extremely well. One example of the quality of the fit is shown in Figure 4. Visible is the measured and simulated system frequency response (amplitude $|\underline{H}(\Omega)|$ and phase $\psi(\Omega)$) of the absorber prototype due to base excitation with a constant amplitude and 4000 V applied to either channel 1 (a) or channel 2 (b). For comparison, the best linear model is shown as well (dotted line). Varying the applied voltage can alter the resonance

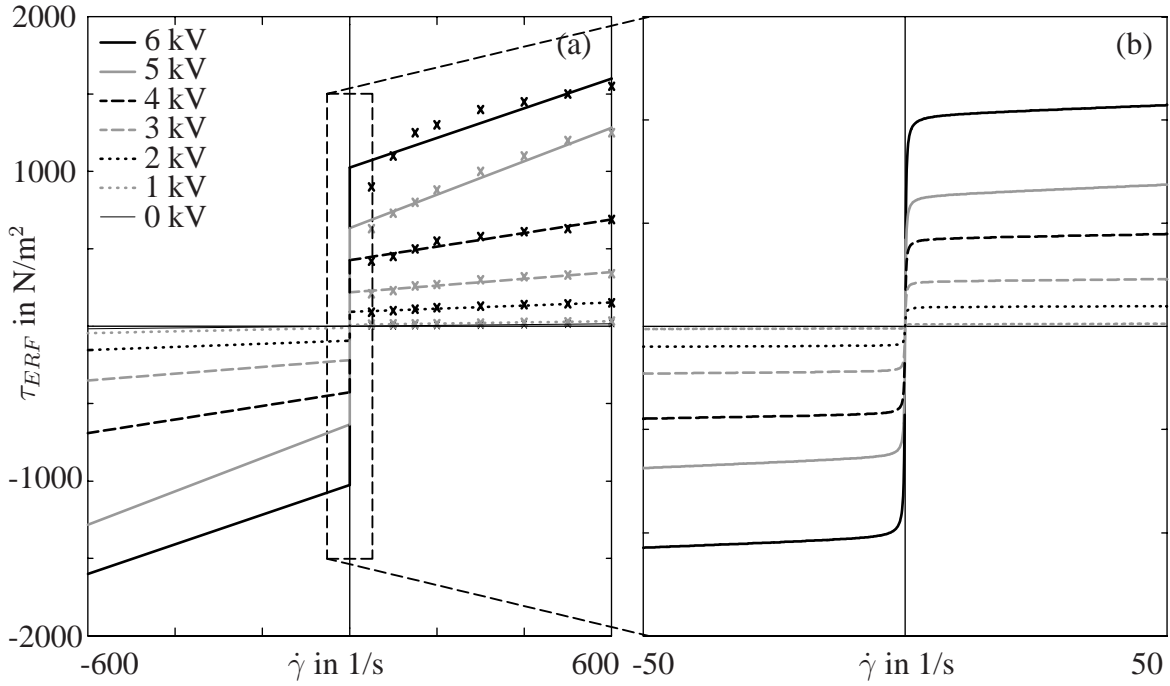


Figure 3: Shear stress due to shear rate with BINGHAM-type model (a) and zoom of the interesting area showing the effect of multiplication with the arctan-function (b)

frequency between 19 and 24 Hz. This can be seen in the measured frequency response curves for increasing voltages in Figure 5. The drop in the resonance frequency from 0 V to 2000 V is due to a change in the added mass of the ERF. From there on, an increase in high voltage results in an increased resonance frequency.

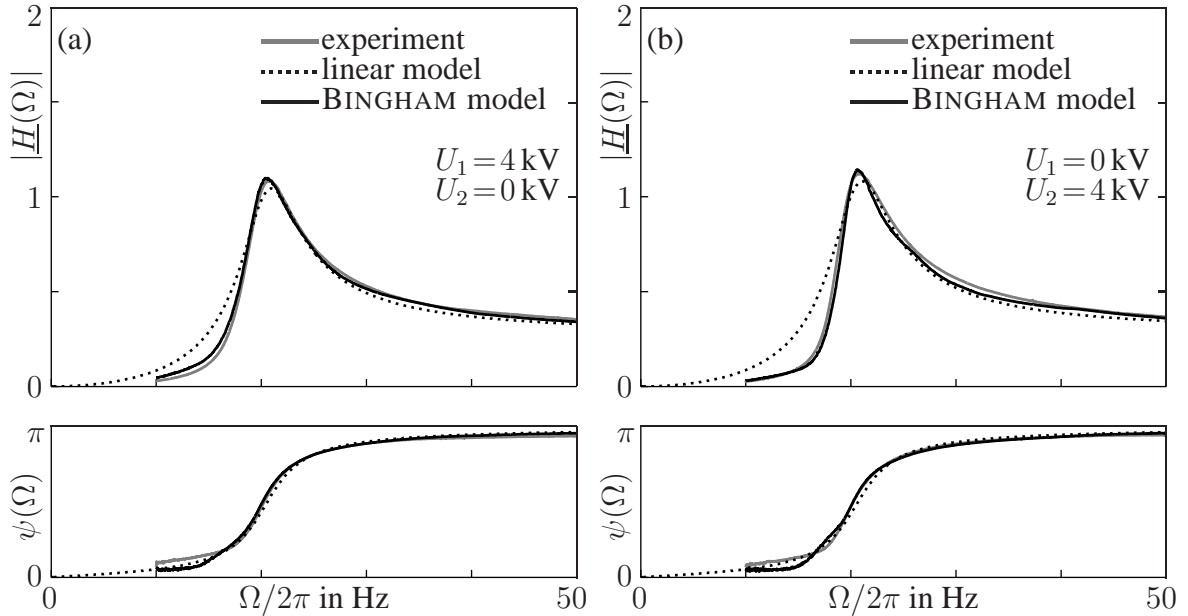


Figure 4: Measured and simulated displacement amplitude $|\underline{H}(\Omega)|$ and phase $\psi(\Omega)$ for the absorber prototype due to base excitation, $U_1 = 4 \text{ kV}$ (a) and $U_2 = 4 \text{ kV}$ (b)

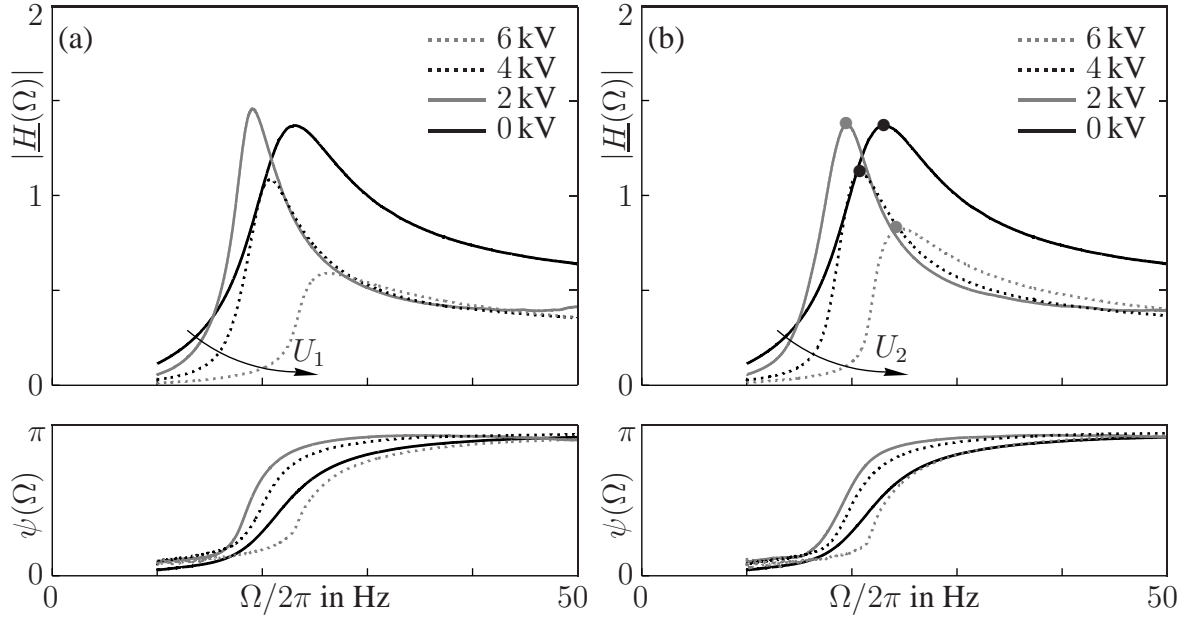


Figure 5: Measured displacement amplitude $|\underline{H}(\Omega)|$ and phase $\psi(\Omega)$ for the absorber prototype due to base excitation, $U_1 = 0$ to 6 kV (a) and $U_2 = 0$ to 6 kV (b)

4 POWER DISSIPATION IN THE ERF

The power dissipation in the ERF cannot be measured, but can be calculated from the hysteretic force-displacement diagrams created with the validated model. We will discuss two cases:

Case 1: The vibration absorber is tuned to a varying excitation frequency via high voltage U_2 . The base excitation amplitude u is assumed to be constant. The points of operation are marked with bullets (\bullet) in Figure 5 (b).

Case 2: The vibration absorber is subjected to a fixed excitation frequency of $\Omega/2\pi = 30$ Hz. The applied high voltage U_2 is increased from 0 to 6000 V.

Figure 6 shows the calculated force-displacement and force-velocity characteristic obtained from the extended BINGHAM-type model for **Case 1**. In this case, the system parameters and excitation frequency change from one voltage to the next, so the displacement q_r of the absorber body is diminished with rising voltages.

Figure 7 shows the calculated force-displacement and force-velocity characteristic obtained from the extended BINGHAM-type model for **Case 2**. For this parameter set, the system response amplitude remains nearly constant with the exception of a change in system behavior from linear (no voltage applied) to non-linear (high voltage applied). The damping work per cycle increases visibly.

From these two diagrams, the damping power for these different points of operation is calculated and shown in Figure 8. The quadratic trend of the data for **Case 2** is due to Eq. (3). This trend is not evident in the data for **Case 1** because of the aforementioned change in the displacement q_r .

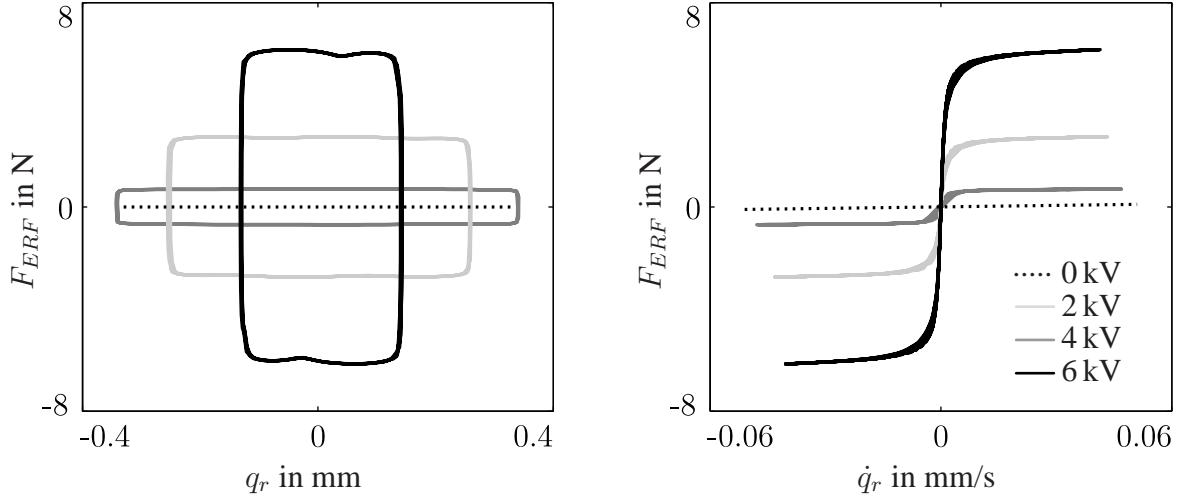


Figure 6: **Case 1:** Calculated force-displacement and force-velocity diagrams for the ERF, high voltages U_2 from 0 to 6000 V applied, harmonic excitation at resonance frequency

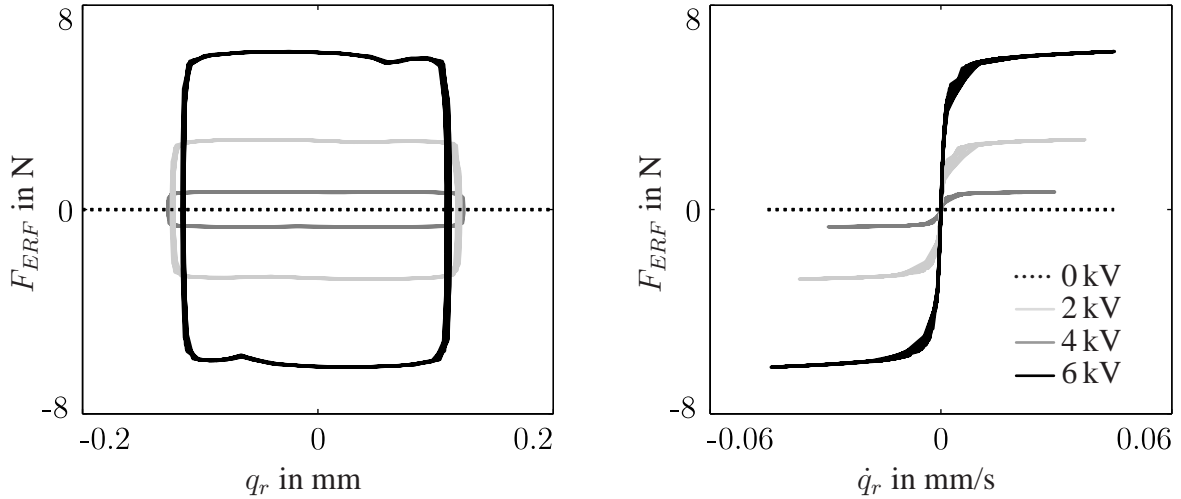


Figure 7: **Case 2:** Calculated force-displacement and force-velocity diagrams for the ERF, high voltages U_2 from 0 to 6000 V applied, harmonic excitation at fixed frequency $\Omega/2\pi = 30$ Hz

5 POWER CONSUMPTION OF THE SEMI-ACTIVE SYSTEM

The power needed to create the electrical fields is very low. Because the ERF is an insulator, the currents flowing through the material are of the order 1 mA. This can be verified by measuring the electrical current during operation with different high voltages. The utilized laboratory-grade high voltage amplifiers support both voltage and current monitoring. The power consumption for steady-state, direct current operation can be calculated simply as the product of voltage and current,

$$P = UI = \frac{U^2}{R}. \quad (5)$$

If the resistance of the ERF is assumed to remain constant, the power consumption will be proportional to the square of the applied voltage.

In addition to the power requirements of the ERF itself, the total power consumed by the high voltage generators coming from the power grid is measured simultaneously with a com-

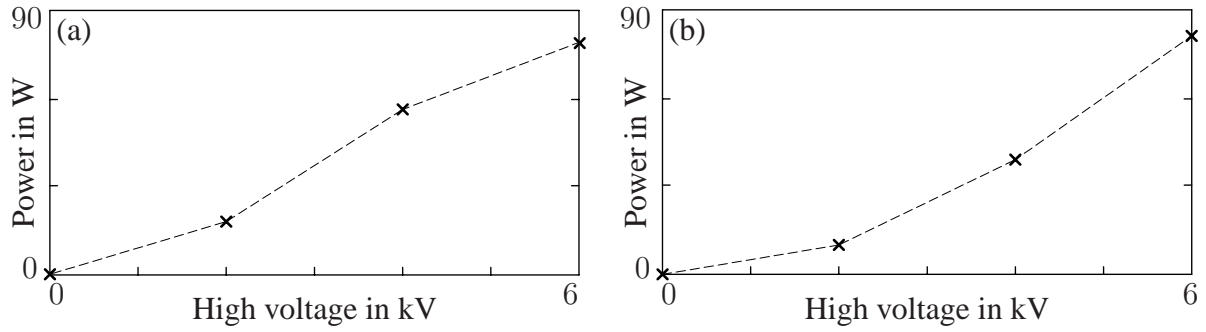


Figure 8: Calculated power dissipation in the ERF in W, **Case 1** (a) and **Case 2** (b)

mercially available wattmeter. The result of this experiment for different high voltages is shown in Figure 9.

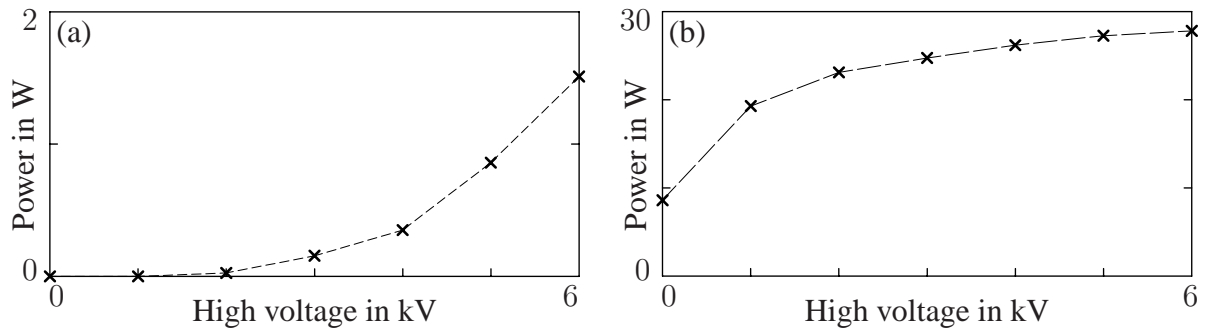


Figure 9: Power consumption of the ERF in W (a) and power consumption of the high voltage generator in W (b)

As expected, the power consumption of the ERF is proportional to the square of the applied voltage. Even when 6000 V are applied, only 2 W of power are needed to maintain the electric field. Comparison with the 80 W of dissipated power results in a amplification factor of 40.

On the other hand, the high voltage generator has a much higher power consumption. In standby the high voltage generator already demands 8.6 W. When 6000 V are applied, the power consumption reaches almost 30 W. The efficiency of the high voltage generator used here is below 6%. With the additional power needed in a complete semi-active system for sensor and controller, the overall efficiency is too low to result in a semi-active absorber with energetic advantages over active systems. For a real industrial application, an optimized high voltage generator is required.

6 CONCLUSIONS

The objective of this paper was to discuss the efficiency of ER material as a semi-active tuning mechanism. The tunable vibration absorber shown here requires very little power compared to the damping evoked by the change in ER material behavior. Measurements of power consumption and numerical results for the corresponding power dissipation were presented. It was shown that the efficiency of the high voltage generators used in this study is too low for the semi-active absorber to exhibit its full potential. Some of the power requirements of the high voltage generator are to be attributed to the different functions and voltage and current monitors supplied by the laboratory unit used for these measurements. These results can help foster further developments of adaptive devices utilizing ERF as an adjustment mechanism.

7 ACKNOWLEDGEMENTS

The author would like to thank Prof. Dr.-Ing. Richard Markert for the fruitful discussions and his constant encouragement and support. Additionally, a special thanks goes to the companies TRW Automotive GmbH and Fludicon GmbH for their support of this research.

REFERENCES

- [1] J. P. Den Hartog, *Mechanical Vibrations*. McGraw-Hill, 1956.
- [2] A. Preumont, *Vibration Control of Active Structures, SMIA 179*. Springer-Verlag Berlin Heidelberg, 2011.
- [3] D. Hrovat, P. Barak and M. Rabins, Semi-Active versus Passive or Active Tuned Mass Dampers for Structural Control *Journal of Engineering Mechanics* **109**, 691–705, 1983.
- [4] W. Winslow, *Method and means for translating electrical impulses into mechanical force*, U.S. Patent No. 2,417,850, 1947.
- [5] W. Winslow, Induced fibrillation of suspensions. *Journal of Applied Physics* **20**, 1137–1140, 1949.
- [6] W. A. Bullough and M. B. Foxon, A proportionate coulomb and viscously damped isolation system. *Journal of Sound and Vibration* **56**(1), 35–44, 1978.
- [7] N. D. Sims, N. J. Holmes and R. Stanway, A unified modelling and model updating procedure for electrorheological and magnetorheological vibration dampers. *Smart Materials and Structures* **13**(1), 100–121, 2004.
- [8] H. Janocha and D. J. Jendritza, Einsatzpotential von Elektrorheologischen Flüssigkeiten. *Konstruktion* **46**, 111–115, 1994.
- [9] T. D. Truong and S. E. Semercigil, A Variable Damping Tuned Absorber with Electro-Rheological Fluid for Transient Resonance of Light Structures. *Journal of Sound and Vibration* **239**(5), 891–905, 2001.
- [10] D. Sakamoto, N. Oshima and T. Fukuda, Tuned sloshing damper using electro-rheological fluid. *Smart Materials and Structures* **10**(5), 963–969, 2001.
- [11] J.-H. Koo, *Using Magneto-Rheological Dampers in Semiactive Tuned Vibration Absorbers to Control Structural Vibrations*. PhD thesis, Virginia Polytechnic Institute and State University, 2003.
- [12] M. H. Holdhusen, *The State-Switched Absorber Used for Vibration Control of Continuous Systems*. PhD thesis, Georgia Institute of Technology, 2005.
- [13] C. Hirunyapruk, *Vibration Control Using an Adaptive Tuned Magneto-Rheological Fluid Vibration Absorber*. PhD thesis, University of Southampton, 2009.
- [14] N. Norrick, R. Markert and D. Plöger, *VDI-Berichte Nr. 2093*, 73–81, 2010.

- [15] N. Norrick, R. Markert and R. Nicoletti, *XIV International Symposium on Dynamic Problems of Mechanics (DINAME 2011)*, Maresias, Brasil, 2011.
- [16] Z. Huang and J. H. Spurk, Der elektroviskose Effekt als Folge elektrostatischer Kraft. *Rheologica Acta* **29** (5), 475–481, 1990.
- [17] J. Bauer, *Intelligenter ERF-Schwingungsdämpfer für Rotorsysteme mit großen Amplituden*. Fortschritt-Berichte VDI: Reihe 11 Band 346, VDI-Verlag Düsseldorf, 2012.
- [18] N. Norrick, *Elektrorheologisch verstellbare Mehrfreiheitsgrad-Schwingungstilger*. Fortschritt-Berichte VDI: Reihe 11 Band 347, VDI-Verlag Düsseldorf, 2013.